Microchimica Acta (2019) 186:569
https://doi.org/10.1007/s00604-019-3672-6

ORIGINAL PAPER

Amperometric biosensor for glyphosate based on the inhibition of tyrosinase conjugated to carbon nano-onions in a chitosan matrix on a screen-printed electrode

Vibol Sok[1] · Alex Fragoso[1]

Received: 19 March 2019 / Accepted: 6 July 2019

Abstract
Glyphosate [N-(phosphonomethyl)glycine] is the most frequently used herbicide to date. Due to its indiscriminate use, it has become a globally occurring pollutant of surface waters. A biosensor for glyphosate is described here that consists of a carbon nano-onion/tyrosinase conjugate immobilized in a chitosan matrix on a screen-printed electrode. The analytical principle is based on the inhibition of the enzyme tyrosinase by glyphosate. L-DOPA is used as the enzyme substrate. The presence of the carbon nano-onions has a beneficial effect on the sensitivity of the assay. Glyphosate can be amperometrically quantified in the 0.015 to 10 μM concentration range and with a 6.5 nM (1.1 μg L^{-1}) detection limit. The biosensor is stable more than 2 months at 4 °C. It was applied to the detection of glyphosate in water and soil samples taken from irrigation of a rice field after aerial application. Results were in good agreement with data obtained by a commercial ELISA.

Keywords Nanomaterial · Herbicide · Pollutant · Contamination · Rice · Soil · Water · Irrigation · ELISA

Introduction

Glyphosate [*N*-(phosphonomethyl)glycine)] is a frequently used organophosphorous herbicide [1]. It has become a globally occurring pollutant in surface water because of its good solubility and slow degradation. Regulatory rules to limit the presence of glyphosate in water and plants differ significantly from country to country. For example, the maximum glyphosate level in drinking water allowed in the United States is 700 μg L^{-1} while in the European Union this concentration is 0.1 μg L^{-1} [2]. Several methods are available for glyphosate detection in plant, soil and water samples. Among them, chromatographic, spectroscopic and enzyme-linked immunosorbent techniques are the most commonly used [3]. They provide a good sensitivity but are slow and expensive techniques and often require sample pre-treatment. To circumvent these drawbacks, enzymatic biosensors have emerged as useful tools for herbicide and pesticide detection at low concentrations. These biosensors operate using an inhibition mechanism and several pesticides have been detected based on this principle [4–10]. They are easy to use and can be regenerated and reused but care should be taken to ensure the adequate selectivity and specificity of the measurements. This can be achieved using separation steps and/or devising novel transducer modification strategies that isolate the target analyte over the interferences [11].

Carbon nanomaterials have emerged as one of the most suitable materials in biosensing [12]. Their combination of interfacial and electric properties makes them very attractive candidates for transducer modification in electrochemical biosensorss [3, 13–15]. We have exploited the modification of electrode surfaces with carbon nano-onions (CNOs) in the construction of electrochemical DNA sensors [16] and as supports for enzyme immobilization [17]. CNOs are hollow spherical nanoparticles formed concentric graphene layers with increasing diameters and show a rather unique combination of high surface-to-volume ratio, high conductivity, thermal stability and biocompatibility [18, 19]. They can be easily modified by a wide range of functional groups and incorporated in composite materials with organic or inorganic polymers for a wide range of applications including energy storage, bioimaging, sensing, etc. [20].

✉ Alex Fragoso
alex.fragoso@urv.cat

[1] Nanobiotechnology & Bioanalysis Group, Departament d'Enginyeria Química, Universitat Rovira i Virgili, Avinguda Països Catalans 26, 43007 Tarragona, Spain

Published online: 24 July 2019

Here we report on the preparation of a CNO/TYR conjugate and its incorporation in a chitosan (Chit) matrix with the aim to develop an amperometric biosensor for glyphosate. Detection is based on the inhibition of tyrosinase activity, which, to the best of our knowledge, has not been used for the detection of this important herbicide. We study the effect of the CNOs on the analytical parameters and stability of the constructed biosensor and apply it to the detection of glyphosate in soil and water samples taken from irrigation of a rice field before and after aerial application of glyphosate.

Experimental

Materials and reagents

All chemicals and solvents were used as received. Oxidized CNOs were prepared by oxidation of CNOs (100 mg) with 10 mL of HNO_3/H_2SO_4 (1:3 *v*/v) for one hour at room temperature [17]. EDC, NHS, glyphosate, chitosan (average Mw 5 kDa, 91% deacetylation), phosphate buffered saline (PBS), tyrosinase from mushroom (1000 units mg^{-1}) and 3,4-dihydroxy-L-phenylalanine (L-DOPA) were purchased from Sigma-Aldrich (http://www.sigmaaldrich.com/). Screen-printed electrodes (DRP-110) were purchased from Metrohm DropSens (http://www.dropsens.com/). All solutions were prepared with water purified using a Milli-Q water purification system (Millipore) to a resistivity of 18.2 MΩ·cm.

Instrumentation

Environmental Scanning Electron Microscopy (ESEM) was recorded in a Quanta 600 microscope (FEI Company Inc.) under high vacuum at 25 kV. All electrochemical measurements were carried out using an Autolab model PGSTAT 10 potentiostat/galvanostat controlled with the general purpose electrochemical systems (GPES) software (Eco Chemie, the Netherlands), equipped with a cable connector for screen-printed electrode (DRP-CAC, from Metrohm DropSens). Cyclic voltammetry studies were conducted in degassed buffers at a scan rate of 100 mV s^{-1}.

Biosensor preparation

Prior to modification, the bare screen-printed electrodes were cleaned/activated with 1 M H_2SO_4 using cyclic voltammetry in the potential range − 0.5 to 1.0 V at 0.1 V s^{-1} for 10 cycles. Chitosan solution (1%) was prepared in 0.8% acetic acid with 3 h stirring at room temperature. The coating solution was prepared as follows: 1.2 mg of TYR and 0.25 mg of ox-CNO were mixed with 1 mg EDC and 2 mg NHS in 200 μL acetate buffer pH 5 and stirred at 4 °C for 4 h. The mixture was filtered through a 100 kDa Amicon® centrifugal filter and the retentate (30 μL) was mixed with 200 μL of 1% chitosan. After stirring overnight at 4 °C, 2 μL of this solution were dropped on the surface of the SPEs and dried under vacuum for 2 h (SPE/Chi/CNO/TYR electrodes).

Control electrodes (SPE/Chi/TYR) were prepared in a similar way but without CNOs. One mg of TYR was activated with 1 mg EDC and 2 mg NHS for 4 h at 4 °C in 50 μL acetate buffer pH 5. This solution was mixed with 30 μL of 1% chitosan and stirred overnight. The activity of the conjugate solution was measured spectrophotometrically in order to ensure that both types of electrodes contained the same amount of immobilized tyrosinase. Finally, 1.5 μL of this solution were dropped on the surface of the SPEs and dried under vacuum for 2 h (SPE/Chi/Tyr). The electrodes were stored in 20 mM PBS in the fridge when not in use.

Biosensor characterization and detection procedures

The electrochemical behavior of the biosensors was investigated by CV in the potential range of −0.3 to +0.6 V with scan rate 100 mV s^{-1} in 20 mM PBS pH 7 and 1 mM $K_3[Fe(CN)_6]$ in 0.1 mM KCl or 10 mM of L-DOPA in 20 mM PBS pH 7.

Inhibition measurements were carried out in a two-step process. Two solutions of the same concentration of glyphosate were prepared, one without substrate for biosensor incubation and another one with substrate for the amperometric measurements after sample incubation. The initial response of the non-inhibited biosensor (A_0) was first recorded, followed by incubation in the presence of glyphosate (A_i). After rinsing, the residual activity was then measured and the % of inhibition was calculated according using the equation $\%I = (A_0 - Ai)/A_0 \times 100$. The DC amperometric measurements were carried out in stirred electrolytes (425 rpm) at an applied potential of −0.20 V vs. Ag/AgCl in a solution containing 1.5 mM of L-DOPA. All measurements were carried out in triplicate.

Real sample analysis and stability study

The irrigation water samples with a pH of 7.2 were filtered through a 0.22 μm syringe filter and analyzed as described before without any further treatment. The soil sample (previously dried at 100 °C overnight) was homogenized manually before extraction. Glyphosate was extracted from soil by treating 1 g of solid with 5 mL of KOH 0.6 M for 1 h. After centrifugation at 5000 rpm for 10 min, the pH of the supernatant was adjusted to 7 with 470 μL of HCl 6 M and the aqueous sample was analyzed as described before. The glyphosate contents in the solid sample was expressed in μg g^{-1}. In both cases the results were compared with those obtained using an ELISA kit (Abnova) following the instructions of the manufacturer. The samples were analyzed in triplicate.

The stability of the biosensors stored in the fridge in PBS at 4 °C was studied by measuring the inhibition of enzyme activity in the presence of 1 μM glyphosate. Repeatability was studied in three identical electrodes by repeated measurement of the enzyme activity until the signal decreased by 10% with respect to the original signal for the above glyphosate concentration.

Results and discussion

Characterization of the modified electrodes

Chitosan is a natural polyaminosaccharide that has been widely used as a platform for enzyme immobilization in industrial and biosensing applications. It forms permeable membranes and is chemically reactive due to the many amino groups present in the structure [21] (Fig. 1). To prepare the biosensor, a CNO/TYR conjugate was first prepared by covalent attachment of the enzyme to the carboxylic acid groups of ox-CNO. This conjugate contained an average of 2 TYR molecules per CNO as determined by thermogravimetric analysis [17] (Fig. 2a) and was further cross-linked with chitosan to form the coating mixture. TEM images of the Chi/CNO/TYR composite show a network-like distribution of the CNO/TYR nanoparticles in the chitosan matrix (Fig. 2b). The surface of SPE/Chi/CNO/TYR electrodes show a rough morphology due to the presence of the CNOs (Fig. 2c). The composite completely covers the electrode surface and forms thin films with a thickness of ~3 μm, as determined by ESEM. The surface of the SPE/Chi/TYR electrode consists of superimposed thin layers corresponding to the chitosan membrane and is markedly less rough than the CNO-containing surface (Fig. 2d).

Figure 3a (inset) shows the cyclic voltammograms of bare and modified electrodes using PBS as supporting electrolyte.

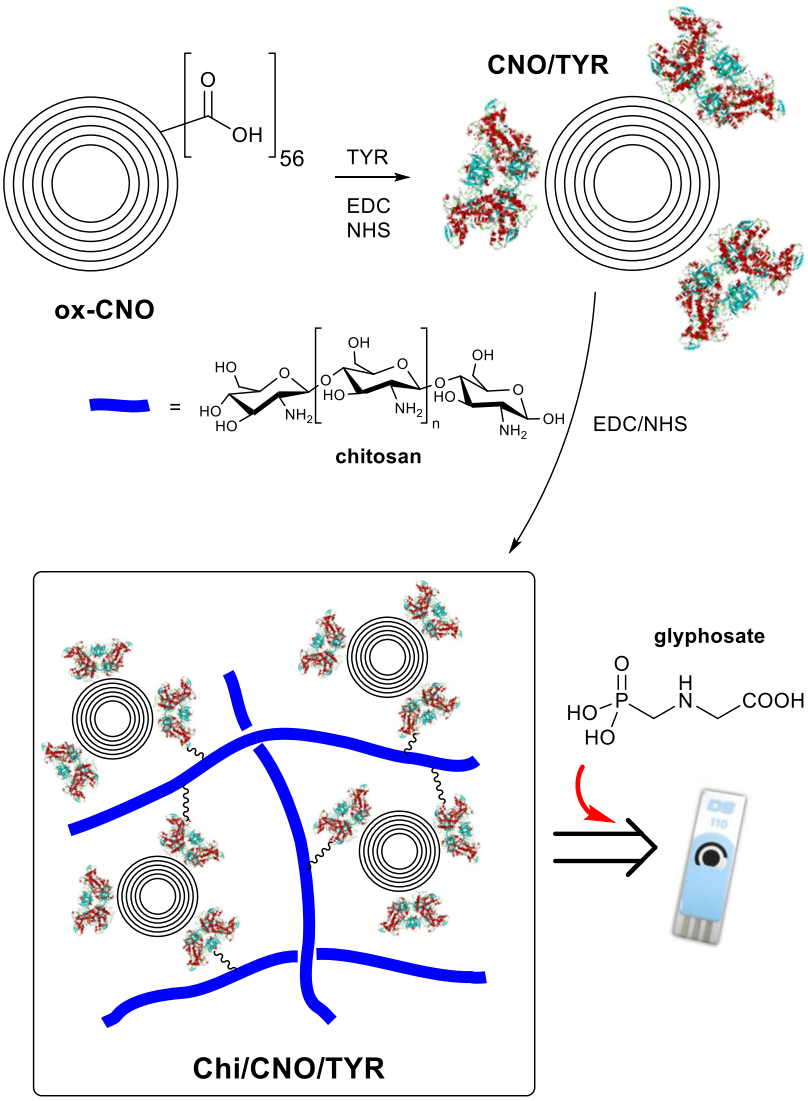

Fig. 1 Preparation of SPE/Chi/CNO/TYR electrodes and structure of glyphosate

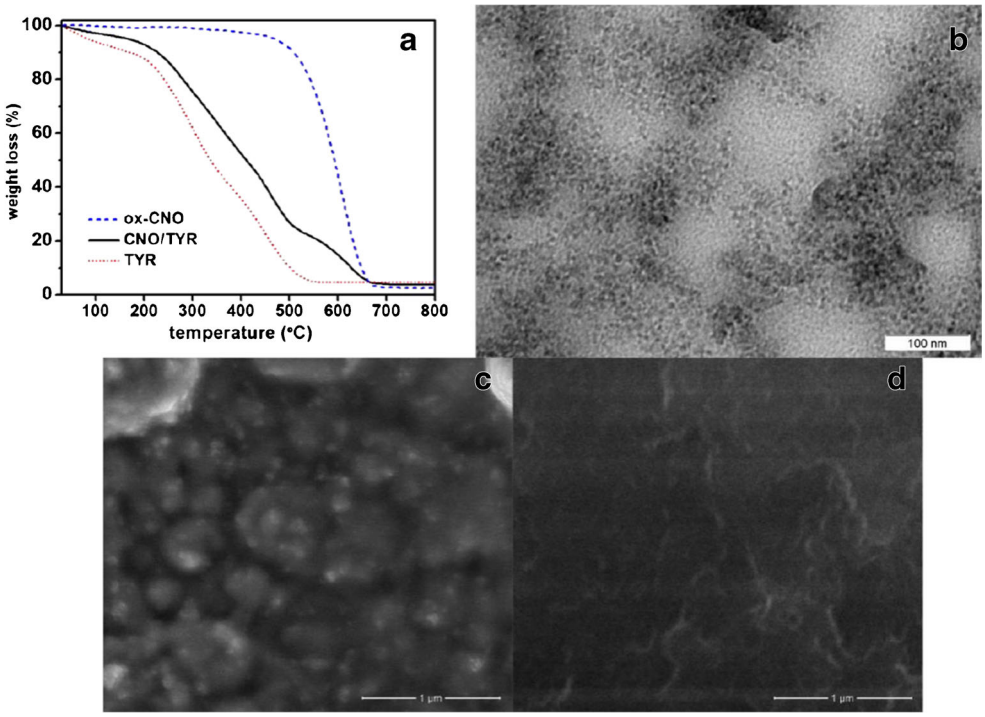

Fig. 2 **a** TGA traces of ox-CNO, CNO/TYR and native TYR. **b** TEM image of the Chi/CNO/TYR composite prior to deposition on the SPEs. **c** ESEM image of SPE/Chi/CNO/TYR and **d** SPE/Chi/TYR

The rectangular shape of the CVs of the modified electrodes is indicative of the deposition of the Chi/CNO layer, which behaves as a pseudocapacitor due to its porous and polyelectrolytic nature. This effect is increased upon incorporation of the CNOs, as reported for other CNO-modified surfaces [16, 22]. The calculated electroactive surface of SPE/Chi/CNO/TYR was 0.775 cm^2 where SPE and SPE/Chi/TYR have surface areas 0.484 and 0.561 cm^2, respectively, as determined by the Randles-Sevcik equation using $[Fe(CN)_6]^{3-}$ in KCl as electroactive marker. These results indicate that the presence of the Chi/CNO/TYR composite improves the active surface of the electrodes thus enhancing the electrochemical properties of the surface. Figure 3a shows the CVs of SPE, SPE/Chi/TYR and SPE/Chi/CNO/TYR in the presence of L-DOPA. In the range of studied potentials, two peak currents appeared in both oxidation and reduction sweeps. At the bare electrode, these pairs of peaks are resolved while in the modified electrodes the peaks are broad. The intensity of the peaks increases in the order SPE > SPE/Chi/TYR > SPE/Chi/CNO/TYR and the peak potentials in the reduction sweep are displaced to more positive potentials, making the redox process more reversible. As expected, the L-DOPA peak potentials are pH-dependent with a slope of 54 mV for the SPE/Chi/CNO/TYR electrodes (Fig. 3b). All these features indicate that both composites are permeable to the enzyme substrate and their electroactive properties are favored with respect to the bare electrode, presumably due to an interfacial accumulation mechanism and the presence of the conductive CNOs.

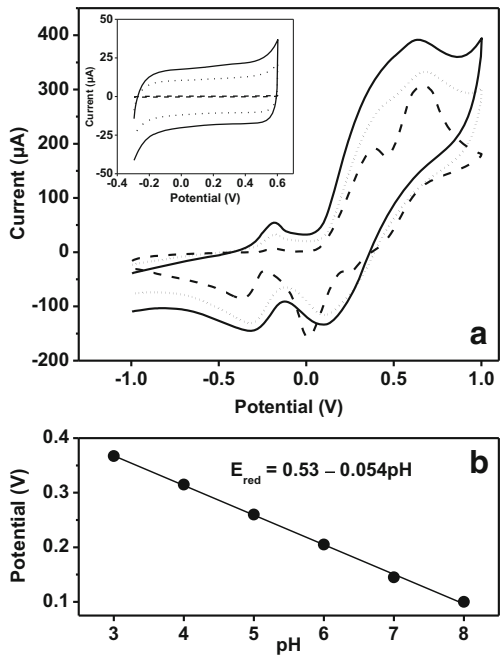

Fig. 3 **a** Cyclic voltammograms of SPE (—), SPE/Chi/TYR (·····) and SPE/Chi/CNO/TYR (——) in the presence of 10 mM L-DOPA in PBS pH 7. Inset: Cyclic voltammograms of SPE (—), SPE/Chi/TYR (·····) and SPE/Chi/CNO/TYR (——) in PBS pH 7. Scan rate: 0.1 V s^{-1}. **b** Dependence of the reduction potential of L-DOPA with pH for the SPE/Chi/CNO/TYR electrodes

Optimization of experimental conditions

Figure 4a shows the amperometric responses of the prepared biosensors at different L-DOPA concentrations. The maximum current is achieved at 1.4 mM of L-DOPA for both TYR

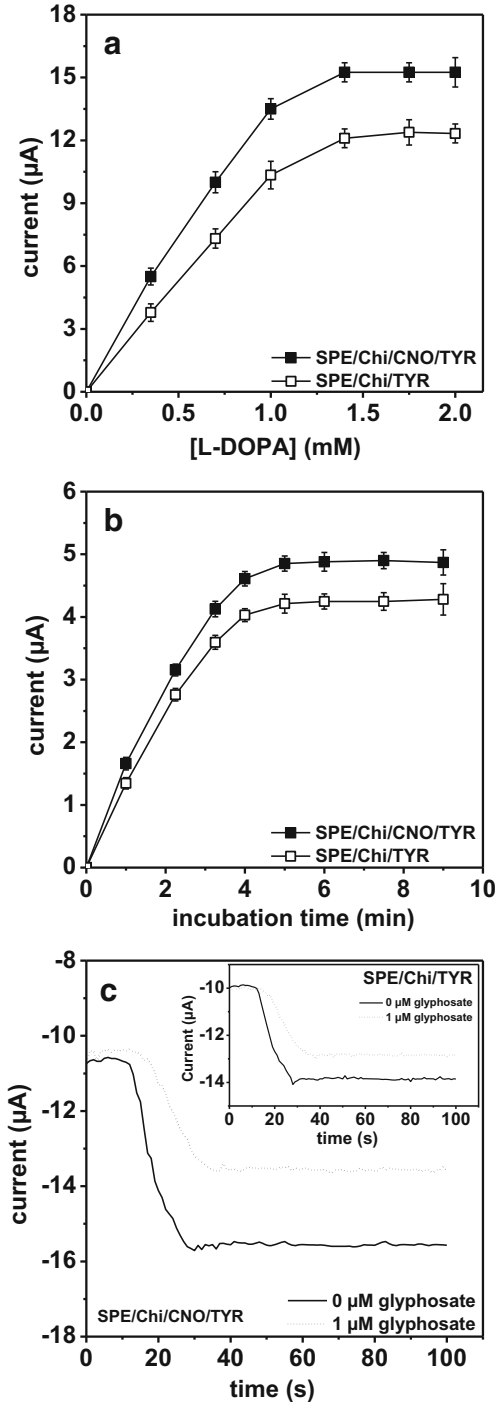

Fig. 4 **a** Amperometric responses of SPE/Chi/CNO/TYR and SPE/Chi/TYR biosensors with different concentrations of L-DOPA in 20 mM 20 mM PBS pH 7. **b** Current variations of SPE/Chi/CNO/TYR and SPE/Chi/TYR in 3.4 μM of glyphosate at different incubation times. Conditions as in a). **c** Amperometric responses at −0.2 V vs. Ag/AgCl of SPE/Chi/CNO/TYR and SPE/Chi/TYR biosensors to 0 and 1 μM of glyphosate in 20 mM PBS pH 7. [L-DOPA] = 0.4 mM

biosensors. Above this concentration, L-DOPA started to saturate the active enzymes of the biosensors to reach maximum activity, as expected for a Michaelis-Menten kinetics. The K_m value of the immobilized tyrosinase was estimated to be 0.81 mM for both biosensors, which is similar to the value reported for the free enzyme (0.78 mM) [23]. This means that the affinity of the enzyme for the substrate is not greatly altered upon immobilization. Interestingly, the calculated K_m values did not depend on the presence of CNOs in the composite.

Another important parameter to optimize in this type of systems is the time the biosensors are kept in contact with the target analyte that behaves as an inhibitor. We have demonstrated that glyphosate is a mixed competitive inhibitor of tyrosinase activity [24]. Thus, inhibitor and substrate compete for the active site of the enzyme and, for a constant substrate concentration, the activity decreases with increasing inhibitor concentration. In solution, this process is typically very fast but with immobilized enzymes in a rather complex matrix some time is needed to complete the diffusion of the reagents. Figure 4b shows the current decrease at increasing glyphosate incubation times for SPE/Chi/TYR and SPE/Chi/CNO/TYR. As seen in the figure, the biosensors need ~5 min to achieve maximum response.

Figure 4c shows the current progress vs. time in the absence and presence of 1 μM glyphosate. As can be seen, the steady-state current started about 60 s after exposing the biosensors into the substrate solution and the current response remained stable for several minutes. Hence, the biosensors were incubated for 1 min after substrate addition before reading the amperometric signal.

Amperometric detection of glyphosate on SPE/Chi/CNO/TYR and SPE/Chi/TYR

The reversible nature of the inhibition mechanism of glyphosate on the catalytic activity of tyrosinase allowed the design of a two-step detection approach that takes into consideration the heterogeneous nature of the enzyme-containing surface in

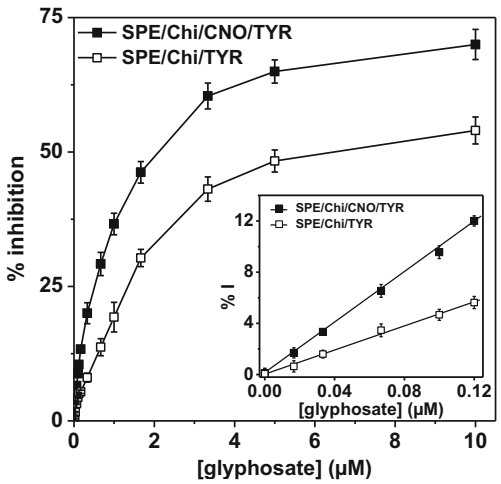

Fig. 5 Calibration plots for SPE/Chi/CNO/TYR and SPE/Chi/TYR at different glyphosate concentrations

Table 1 Comparison of biosensors reported for glyphosate

Surface chemistry	Detection technique	LOD	Reference
HRP adsorbed on PDMS/PSS film	Amperometry, enzyme inhibition	1.70 μg L^{-1}	[25]
Peroxidase (from atemoya) on montmorillonite nanoclay modified carbon paste electrode	Amperometry, enzyme inhibition	30 μg L^{-1}	[26]
Glyphosate-binding oligopeptide on SPR chip	Surface plasmon resonance, direct measurement	97 μg L^{-1}	[27]
HRP-assisted generation of ZnS quantum dots	Electrochemiluminescence, enzyme inhibition	270 μg L^{-1}	[28]
Urease entrapped on agarose-guar gum nanoconjugate	Potentiometric, enzyme inhibition	0.5 μg L^{-1}	[29]
HRP adsorbed on MWCNTs/graphite epoxy	Cyclic voltammetry, enzyme inhibition	1.32 μg L^{-1}	[30]
Molecularly imprinted polymer	Anodic stripping voltammetry	0.35 μg L^{-1}	[31]
Anti-glyphosate antibody immobilized on Si substrate	Fluorescence, competitive inhibition imunoassay	0.04 μg L^{-1}	[32]
Carbon nano-onion/ tyrosinase conjugate on chitosan matrix	Amperometry, enzyme inhibition	1.1 μg L^{-1}	This work

order to achieve the maximum sensitivity. Hence, by measuring the amperometric response of the biosensors in the absence and presence of glyphosate it was possible to construct the corresponding calibration plots based on percentage of signal inhibition.

Figure 5 shows the calibration plots of inhibition of glyphosate on L-DOPA response for SPE/Chi/CNO/TYR and SPE/Chi/TYR biosensors. The plots show that the inhibition percent increases almost linearly with herbicide concentration for both biosensors and then tends slowly to saturation, with the highest *%I* values of ~70%. A linear relationship was found up to 0.12 μM for both biosensors. The detection limits were 6.5 nM (1.1 μg L^{-1}) for SPE/Chi/CNO/TYR and 12 nM (1.9 μg L^{-1}) for SPE/Chi/TYR. In the range of studied concentrations of glyphosate, the sensitivity of the SPE/Chi/CNO/TYR biosensor (taken as the slope of the linear part) was 51.5%μM^{-1}. This value is 2.1 times higher in comparison to SPE/Chi/TYR. The inhibition of glyphosate on TYR in solution was found to be of a mixed competitive type with inhibition constants of 33 μM (K_I) and 183 μM (K_{IS}) for the enzyme and enzyme-L-DOPA complex, respectively [24]. In our case, the SPE/Chi/CNO/TYR contained the enzyme loaded in a CNO-containing composite that enhances electron transfer of the electroactive products, in a similar mechanism to other CNO-based surfaces [16, 22]. On other hand, the SPE/Chi/CNO/TYR has higher surface area compared to SPE/Chi/TYR, in which the enzyme is better distributed on the sensor, making the enzyme with higher capability of sensing toward substrate as well as inhibitors. To the best of our knowledge, this is the first example of a tyrosinase-based biosensor for glyphosate detection, which is more sensitive in comparison to other biosensors previously reported based on HRP (Table 1). It should also be noted that the LOD is well below the maximum contaminant level allowed in the United States (700 μg L^{-1}) although still higher than the maximum admissible concentration in drinking water in the European Union (0.1 μg L^{-1}).

Analysis of real samples

The applicability of the biosensors in real samples was tested using water and soil samples taken from irrigation of a rice field near Guadalquivir River in South Spain before and after aerial application of glyphosate. Table 2 shows the glyphosate levels obtained using the CNO-based biosensor and a commercial ELISA kit. In the case of the soil sample, the

Table 2 Glyphosate concentrations obtained in water and soil samples ($n = 3$)

Sample	Type	Method	Concentration found (μg L^{-1})
1	Irrigation water before glyphosate application	SPE/Chi/CNO/TYR biosensor	0.25 ± 0.06
		ELISA	0.22 ± 0.02
2A	Irrigation water after glyphosate application	SPE/Chi/CNO/TYR biosensor	2.2 ± 0.6
		ELISA	2.06 ± 0.08
2B	Irrigation water after glyphosate application	SPE/Chi/CNO/TYR biosensor	1.9 ± 0.5
		ELISA	1.82 ± 0.03
3	Soil exposed to glyphosate	SPE/Chi/CNO/TYR biosensor	0.9 ± 0.2*
		ELISA	0.83 ± 0.05*

* Values in μg g^{-1}

glyphosate contents is about 1 mg kg^{-1}. This is in the range of the values observed in a recent study of European soil samples and further confirms that agricultural soils absorb important amounts of herbicides and pesticides [33]. In all cases, the values obtained with the biosensors are between 4 and 8% higher than those obtained by ELISA. This indicates that other inhibitors such as glyphosate degradation products may be present in the samples. However, the relatively low differences observed with respect to the standard method suggest that the SPE/Chi/CNO/TYR biosensors can operate in a complex matrix and could find application in agriculture to monitor glyphosate presence.

Biosensor stability and repeatability

The long-term stability and repeatability of the biosensors were examined. Figure 6a shows the residual activities found for the TYR biosensors by monitoring the amperometric responses at a fixed substrate concentration over a period of 4 months. After one month of storage SPE/Chi/CNO/TYR and SPE/Chi/TYR maintain 96% and 77% of their initial activity, respectively, and then decreased gradually to 82% and 38%. In general, from the results of the stability studies of SPE/Chi/CNO/TYR and SPE/Chi/TYR stored in PBS buffer at pH 6.5 and 4 °C it is evident that the presence of CNO in the composite of the SPE/Chi/CNO/TYR biosensor significantly enhanced the stability of the biosensors compared to SPE/Chi/TYR. The increased stability demonstrated for the enzymatic biosensors covalently coupled with CNO is attributed to interparticle interactions between the carbon nanoparticles and the enzyme. This results in a reduction in the enzyme mobility due to the anchorage to the support. Thus, it is shielded it from the denaturing effects of the environment. Interestingly, these results agree with the improved stability observed for CNO-enzyme conjugates in solution [17]. On the other hand, the SPE/Chi/CNO/TYR biosensors maintained a response higher than 90% after 33 measurements (Fig. 6b). These results can also be explained based on the stability of the enzyme conjugates with CNO and the presence of the chitosan matrix.

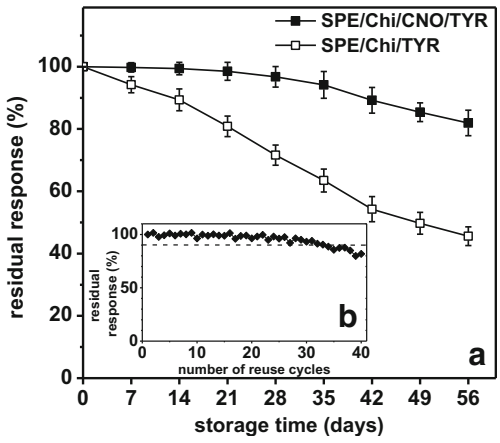

Fig. 6 **a** Residual activities of SPE/Chi/CNO/TYR and SPE/Chi/TYR biosensors stored in 20 mM PBS, pH 6.5 at 4 °C. **b** Residual activity of a SPE/Chi/CNO/TYR biosensor after repeated use (see Experimental section for details)

Conclusions

A highly sensitive biosensor for glyphosate based on the inhibition of tyrosinase activity was prepared by covalent immobilization of an enzyme conjugate on a chitosan matrix. The presence of CNOs on the chitosan-enzyme composites had a positive effect in enhancing the sensitivity of the biosensors due to an increased active surface area combined with enhanced electron transfer properties provided by the conductive nanoparticles. CNOs also proved beneficial to improve their stability and repeatability. Our results demonstrate the feasibility of using chitosan/CNO/enzyme composites for the development of sensitive biosensors based on activity inhibition. It is expected that this strategy can be extended to other systems.

Acknowledgements VS thanks Generalitat de Catalunya for a predoctoral scholarship (grant 2015FI_B00523). AF thanks Ministerio de Economía y Competitividad, Spain (Grant BIO2012-30936 to AF).

Compliance with ethical standards The author(s) declare that they have no competing interests.

References

1. Farmer D (2010) Inhibitors of aromatic acid biosynthesis. In: Krieger R (ed) Hayes' handbook of pesticide toxicology, 3rd edn. Academic Press, New York, Chapter 92, pp 1967–1972
2. Valle AL, Mello FCC, Alves-Balvedi RP, Rodrigues LP, Goulart LR (2019) Glyphosate detection: methods, needs and challenges. Environ Chem Lett 17:291–231. https://doi.org/10.1007/s10311-018-0789-5
3. Gauglitz G, Wimmer B, Melzer T, Huhn C (2017) Glyphosate analysis using sensors and electromigration separation techniques as alternatives to gas or liquid chromatography. Anal Bioanal Chem 410:725–746. https://doi.org/10.1007/s00216-017-0679-x
4. Vidal JC, Esteban S, Gil J, Castillo JR (2006) A comparative study of immobilization methods of a tyrosinase enzyme on electrodes and their application to the detection of dichlorvos organophosphorus insecticide. Talanta 68:791–799. https://doi.org/10.1016/j.talanta.2005.06.038
5. Tanimoto de Albuquerque YD, Ferreira LF (2007) Amperometric biosensing of carbamate and organophosphate pesticides utilizing screen-printed tyrosinase-modified electrodes. Anal Chim Acta 596:210–221. https://doi.org/10.1016/j.aca.2007.06.013
6. Campanella L, Lelo D, Martini E, Tomassetti M (2007) Organophosphorus and carbamate pesticide analysis using an inhibition tyrosinase organic phase enzyme sensor; comparison by butyrylcholinesterase+choline oxidase opee and application to natural waters. Anal Chim Acta 587:22–32. https://doi.org/10.1016/j.aca.2007.01.023

7. Pita MTP, Reviejo AJ, de Villena FJM, Pingarrón JM (1997) Amperometric selective biosensing of dimethyl- and diethyldithiocarbamates based on inhibition processes in a medium of reversed micelles. Anal Chim Acta 340:89–97. https://doi.org/10.1016/s0003-2670(96)00552-1
8. de Lima F, Lucca BG, Barbosa AMJ, Ferreira VS, Moccelini SK, Franzoi AC, Vieira IC (2010) Biosensor based on Pequi polyphenol oxidase immobilized on chitosan crosslinked with cyanuric chloride for thiodicarb determination. Enzym Microb Technol 47:153–158. https://doi.org/10.1016/j.enzmictec.2010.05.006
9. Guan Y, Liu L, Chen C, Kang X, Xie Q (2016) Effective immobilization of tyrosinase via enzyme catalytic polymerization of l -DOPA for highly sensitive phenol and atrazine sensing. Talanta 160:125–132. https://doi.org/10.1016/j.talanta.2016.07.003
10. Mazzei F, Botrè F, Montilla S, Pilloton R, Podestà E, Botrè C (2004) Alkaline phosphatase inhibition based electrochemical sensors for the detection of pesticides. J Electroanal Chem 574:95–100. https://doi.org/10.1016/j.jelechem.2004.08.004
11. Luque de Castro MD, Herrera MC (2003) Enzyme inhibition-based biosensors and biosensing systems: questionable analytical devices. Biosens Bioelectron 18:279–294. https://doi.org/10.1016/S0956-5663(02)00175-6
12. Yang W, Ratinac KR, Ringer SP et al (2010) Carbon nanomaterials in biosensors: should you use nanotubes or graphene? Angew Chem Int Ed 49:2114–2138. https://doi.org/10.1002/anie.200903463
13. Zhao F, Wu J, Ying Y, She Y, Wang J, Ping J (2018) Carbon nanomaterial-enabled pesticide biosensors: design strategy, biosensing mechanism, and practical application. TrAC Trends Anal Chem 106:62–83. https://doi.org/10.1016/j.trac.2018.06.017
14. Yang Q, Qu Y, Bo Y, Wen Y, Huang S (2010) Biosensor for atrazin based on aligned carbon nanotubes modified with glucose oxidase. Microchim Acta 168:197–203. https://doi.org/10.1007/s00604-009-0272-x
15. Ju K-J, Feng J-X, Feng J-J, Zhang QL, Xu TQ, Wei J, Wang AJ (2015) Biosensor for pesticide triazophos based on its inhibition of acetylcholinesterase and using a glassy carbon electrode modified with coral-like gold nanostructures supported on reduced graphene oxide. Microchim Acta 182:2427–2434. https://doi.org/10.1007/s00604-015-1584-7
16. Bartolome JP, Echegoyen L, Fragoso A (2015) Reactive carbon nano-onion modified glassy carbon surfaces as DNA sensors for human papillomavirus oncogene detection with enhanced sensitivity. Anal Chem 87:6744–6751. https://doi.org/10.1021/acs.analchem.5b00924
17. Sok V, Fragoso A (2018) Preparation and characterization of alkaline phosphatase, horseradish peroxidase, and glucose oxidase conjugates with carboxylated carbon nano-onions. Prep Biochem Biotechnol 48:136–143. https://doi.org/10.1080/10826068.2017.1405025
18. Mykhailiv O, Zubyk H, Plonska-Brzezinska ME (2017) Carbon nano-onions: unique carbon nanostructures with fascinating properties and their potential applications. Inorg Chim Acta 468:49–66. https://doi.org/10.1016/j.ica.2017.07.021
19. Camisasca A, Giordani S (2017) Carbon nano-onions in biomedical applications: promising theranostic agents. Inorg Chim Acta 468:67–76. https://doi.org/10.1016/j.ica.2017.06.009
20. Bobrowska DM, Czyrko J, Brzezinski K, Echegoyen L, Plonska-Brzezinska ME (2016) Carbon nano-onion composites: physicochemical characteristics and biological activity. Fullerenes, Nanotubes, Carbon Nanostructures 25:185–192. https://doi.org/10.1080/1536383x.2016.1248758
21. Krajewska B (2004) Application of chitin- and chitosan-based materials for enzyme immobilizations: a review. Enzym Microb Technol 35:126–139. https://doi.org/10.1016/j.enzmictec.2003.12.013
22. Bartolome JP, Fragoso A (2017) Electrochemical detection of nitrite and ascorbic acid at glassy carbon electrodes modified with carbon nano-onions bearing electroactive moieties. Inorg Chim Acta 468:223–231. https://doi.org/10.1016/j.ica.2017.06.024
23. Wu Q, Xu Z, Duan Y, Zhu Y, Ou M, Xu X (2017) Immobilization of tyrosinase on polyacrylonitrile beads: biodegradation of phenol from aqueous solution and the relevant cytotoxicity assessment. RSC Adv 7:28114–28123. https://doi.org/10.1039/c7ra03174b
24. Sok V, Fragoso A (2018) Kinetic, spectroscopic and computational docking study of the inhibitory effect of the pesticides 2,4,5-T, 2,4-D and glyphosate on the diphenolase activity of mushroom tyrosinase. Int J Biol Macromol 118:427–434. https://doi.org/10.1016/j.ijbiomac.2018.06.098
25. Songa EA, Arotiba OA, Owino JHO, Jahed N, Baker PGL, Iwuoha EI (2009) Electrochemical detection of glyphosate herbicide using horseradish peroxidase immobilized on sulfonated polymer matrix. Bioelectrochemistry 75:117–123. https://doi.org/10.1016/j.bioelechem.2009.02.007
26. Oliveira GC, Moccelini SK, Castilho M, Terezo AJ, Possavatz J, Magalhães MRL, Dores EFGC (2012) Biosensor based on atemoya peroxidase immobilised on modified nanoclay for glyphosate biomonitoring. Talanta 98:130–136. https://doi.org/10.1016/j.talanta.2012.06.059
27. Ding X, Yang K-L (2013) Development of an oligopeptide functionalized surface Plasmon resonance biosensor for online detection of glyphosate. Anal Chem 85:5727–5733. https://doi.org/10.1021/ac400273g
28. Zhang Q, Xu G, Gong L, Dai H, Zhang S, Li Y, Lin Y (2015) An enzyme-assisted electrochemiluminescent biosensor developed on order mesoporous carbons substrate for ultrasensitive glyphosate sensing. Electrochim Acta 186:624–630. https://doi.org/10.1016/j.electacta.2015.10.081
29. Vaghela C, Kulkarni M, Haram S, Aiyer R, Karve M (2018) A novel inhibition based biosensor using urease nanoconjugate entrapped biocomposite membrane for potentiometric glyphosate detection. Int J Biol Macromol 108:32–40. https://doi.org/10.1016/j.ijbiomac.2017.11.136
30. Cahuantzi-Muñoz SL, González-Fuentes MA, Ortiz-Frade LA, Torres E, Ţălu Ş, Trejo G, Méndez-Albores A (2019) Electrochemical biosensor for sensitive quantification of glyphosate in maize kernels. Electroanalysis 31:927–935. https://doi.org/10.1002/elan.201800759
31. Prasad BB, Jauhari D, Tiwari MP (2014) Doubly imprinted polymer nanofilm-modified electrochemical sensor for ultra-trace simultaneous analysis of glyphosate and glufosinate. Biosens Bioelectron 59:81–88. https://doi.org/10.1016/j.bios.2014.03.019
32. Lee HU, Jung DU, Lee JH, Song YS, Park C, Kim SW (2013) Detection of glyphosate by quantitative analysis of fluorescence and single DNA using DNA-labeled fluorescent magnetic core–shell nanoparticles. Sensors Actuators B Chem 177:879–886. https://doi.org/10.1016/j.snb.2012.11.075
33. Silva V, Mol HGJ, Zomer P, Tienstra M, Ritsema CJ, Geissen V (2019) Pesticide residues in European agricultural soils – a hidden reality unfolded. Sci Total Environ 653:1532–1545. https://doi.org/10.1016/j.scitotenv.2018.10.441